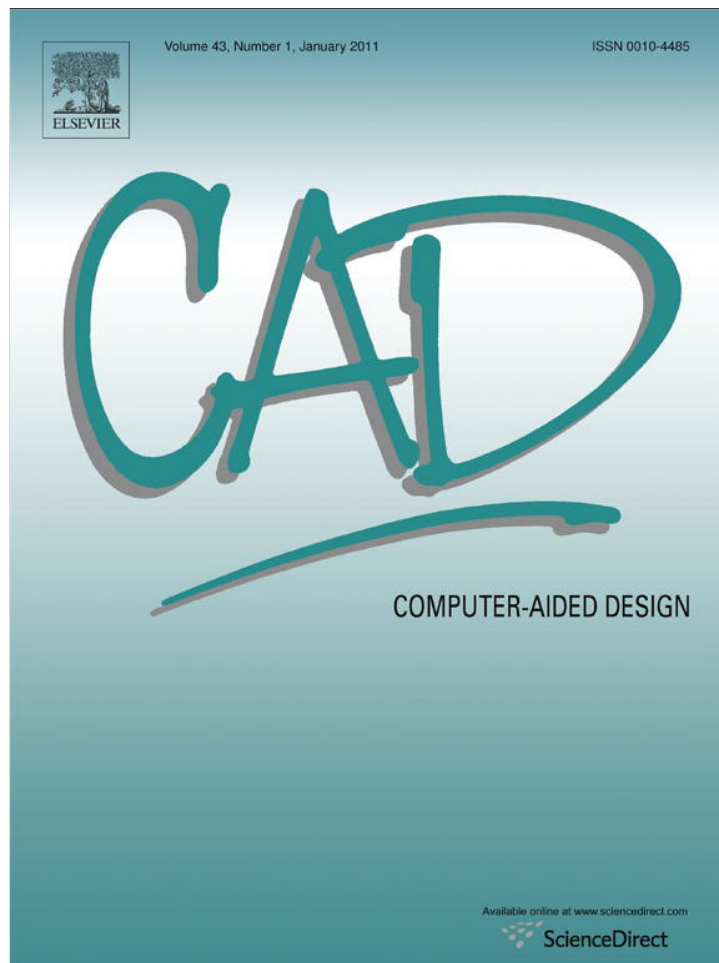


Provided for non-commercial research and education use.
Not for reproduction, distribution or commercial use.



(This is a sample cover image for this issue. The actual cover is not yet available at this time.)

This article appeared in a journal published by Elsevier. The attached copy is furnished to the author for internal non-commercial research and education use, including for instruction at the authors institution and sharing with colleagues.

Other uses, including reproduction and distribution, or selling or licensing copies, or posting to personal, institutional or third party websites are prohibited.

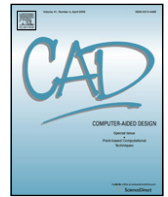
In most cases authors are permitted to post their version of the article (e.g. in Word or Tex form) to their personal website or institutional repository. Authors requiring further information regarding Elsevier's archiving and manuscript policies are encouraged to visit:

<http://www.elsevier.com/copyright>



Contents lists available at ScienceDirect

Computer-Aided Design

journal homepage: www.elsevier.com/locate/cad

Development of hip joint prostheses with modular stems

Ji-Yong Bae^a, Umar Farooque^b, Kyung-won Lee^c, Gyu-Ha Kim^c, Insu Jeon^{a,*}, Taek-Rim Yoon^d^a School of Mechanical Systems Engineering, Chonnam National University, 300 Yongbong-dong, Buk-gu, Gwangju, 500-757, Republic of Korea^b Department of Mechanical Engineering, Indian Institute of Technology Kanpur, Kanpur, 208016, India^c Top Research & Development Co., Ltd., 958-3 Daechon-dong, Buk-gu, Gwangju, 500-706, Republic of Korea^d The Center for Joint Disease, Hwasun Hospital, Chonnam National University, 160 Ilsimri, Hwasun-Eup, Hwasun-Gun, Jeonnam, 519-809, Republic of Korea

ARTICLE INFO

Article history:

Received 3 January 2011

Accepted 10 May 2011

Keywords:

Hip joint replacement
 Minimal invasive surgery
 Prototypical polymer model
 Finite element method
 Ti-6Al-4V modular stem

ABSTRACT

Minimally invasive surgery for THR (Total Hip joint Replacement) is attractive for both surgeons and patients. Since such surgery needs an incision of only 3–4 inches around the hip joint for THR instead of the traditional, large incision of 10–12 inches, it causes less pain and enables early recovery for patients, besides facilitating THR for the operating surgeons. In this research, for minimally invasive THR, a unique type of a cementless stem, named a modular stem, is devised. It consists of two different parts in a stem that can be joined to and separated from each other. For actualizing the modular stem, Bio-CAD modeling technique is applied. The bony structure around the hip joint is three dimensionally reconstructed and its geometric solid model is fabricated. The geometric solid models of modular stems are designed and their prototypical models are fabricated using an acryl-based polymer. The geometric suitability of the prototypical modular stems is manually examined. The strength of the stem to sustain the applied load is evaluated using the finite element method. Finally, various sizes of actual modular stems with circular or rectangular cross-sections are fabricated using a biocompatible Ti alloy (Ti-6Al-4V). The developed modular stems will be used in the near future for minimally invasive THR surgery.

© 2011 Elsevier Ltd. All rights reserved.

1. Introduction

One of the most topical issues in THR (Total Hip joint Replacement) is minimally invasive surgery [1–3]. In reality, it is attractive to both surgeons and patients. In this technique, the replacement of the hip joint is done through an incision of 3–4 in around the hip joint instead of a traditional, large incision of 10–12 in. Such surgery has some definite advantages over traditional methods, such as less pain and early recovery for patients and the facilitation of THR for the operating surgeons.

In practice, this technique necessitates the development of new types of stem. Many different types of stem have been developed until now to fulfill the requirements of minimally invasive surgery for THR. For example, a Birmingham-type stem used in BHR (Birmingham hip resurfacing) arthroplasty [4], a Lubinus SPII stem [5], a Mueller curved stem [5], and a narrow stem with two holes in its shoulder [6] are used in minimally invasive surgery. However, these stems are associated with some problems, such as their limited applicability for severely injured hip joints, surgical

complications with regard to curved stems, the concentration of stress around holes, etc.

To solve these problems, we develop a unique type of modular stem. This stem has a joint around its shoulder and separable parts. Since cemented femoral prostheses recently have been replaced by cementless prostheses for preventing the aseptic loosening of prostheses [7,8], a cementless stem is considered. Actually, different types of modular stem such as the infinity modular hip system [9], the Richards modular hip system [9] and the S-ROM modular hip system [10] have been developed due to off-the-shelf flexibility for customizing proximal and distal canal filling for THR [11]. However, those stems have limitations for minimally invasive surgery due to their geometric shapes and surgical complexities.

For this research, the geometric shape of the modular stem is devised and actualized based on a Bio-CAD modeling technique [12,13]. A three dimensional reconstruction of bony structure around a hip joint and fabrication of its geometric model were carried out. The geometric solid models of modular stems and their prototypical models are fabricated. The strength of the devised stem to sustain the applied load is evaluated using the finite element method. Finally, the modular stem is fabricated using a biocompatible Ti alloy, Ti-6Al-4V. Two different shapes with various sizes of the modular stem with circular or

* Corresponding author. Tel.: +82 62 530 1688; fax: +82 62 530 1689.
 E-mail address: i_jeon@chonnam.ac.kr (I. Jeon).

rectangular cross-sections are fabricated for minimally invasive THR surgery.

2. Bio-CAD modeling and computation

2.1. Initial suggestion of modular stems

The two suggested types of modular stem are designed using the software, CATIA of Dassault Systems. One type of stem has a circular cross-section while the other has a rectangular cross-section. The most interesting feature about these unique types of stem is that each stem has two parts that can be separated or joined with each other. The adequate size and shape of the stem can be decided after considering the shape and size of the cortical and cancellous bones of a patient. For a better fit between the separable ends of each stem, the upper part of the modular stem has a protrusion on the central region of its bottom surface and the lower part has a cavity of the same size and shape as the protrusion on its top surface. The interference fit keeps the two separate parts of the stem in close contact and prevents the relative micromotions and rotations between the two parts.

Each part of the modular stem can be separately implanted into the resected hip joint through a small incision around the hip joint and rejoined together under the implanted state. This process facilitates successful, minimally invasive THR surgery. The designed geometric solid models of both types of modular stem are shown in Fig. 1. Fig. 1(a) shows the stepwise stem with circular cross-section which is devised for preventing the subsidence of the stem into cancellous bone. Fig. 1(b) shows the rectangular cross-section stem with grooves on its surface to give spaces for growth of bone cells.

2.2. Prototypical modular stem models

To actualize our initial idea for the modular stem, first, the prototypical models that can be used for investigating the geometric suitability of the modular stem are fabricated. These models can yield an opportunity for handling the devised stems manually and for checking their shapes from various angles. Also, it is possible to verify the geometric exactness and suitability of the joint of each real model.

The STL output files can be created directly from the solid CAD model and sent to a rapid prototyping machine, viz., Eden 350 of Object Geometries Ltd. From the STL files, thin layers that are 0.1 mm thick are built up one-by-one using the specialized software of the machine until the whole model is formed [14]. The models are fabricated using an acryl-based polymer (Vero white 830). Two fabricated stems, one with a circular cross-section and the other with a rectangular cross-section, are shown in Fig. 2 with their representative sizes. The geometric suitability of the design is confirmed using the models. Note that each stem in Fig. 2(a) and (b) have the fin type thin extrusion on their surfaces for preventing the rotational microdeformation of the stem and micromotion between the stem and the cancellous bone.

2.3. 3D reconstruction of an intact hip joint

To understand completely the stress distribution around the hip joint after THR, a 3D reconstruction of the intact hip joint has been undertaken using X-ray CT (Computed Tomography) images of a subject, who is a 27-year-old woman. Along the axial direction, 446 CT images were taken at intervals of 0.7 mm. Using these images, the sacrum, the left-side coxal bone, and the cortical and cancellous bones of the femur were reconstructed using the commercial software, Mimics version 9.0 (Materialise, Leuven, Belgium) (see [15]).

Table 1

Material properties used for computations.

Materials	Elastic modulus (GPa)	Poisson's ratio	Yield stress (MPa)	Stiffness (N/mm)
Cortical bone	10.5	0.3		
Cancellous bone	0.15	0.2		
Articular cartilage	0.015	0.45		
Stem (Ti-6Al-4V)	110	0.3	970	
Cup (Ti-6Al-4V)	110	0.3	970	
Head (ceramic)	380	0.26		
Liner (UHMWPE)	1.95	0.43		
Gluteii muscles				634
Adductor muscles				344

2.4. Geometric solid modeling and Boolean operations

The geometric solid modeling for each reconstructed model of the intact hip joint has been undertaken through the software, Rapidform 2006 (Inus Technology Inc., Seoul, Korea). In order to reduce the degree of difficulty of whole solid modeling, only one half of the sacrum is selected after considering the symmetric structure of the lower extremity. Also, the actual structure of the sacrum with sacral holes was simplified as a structure without holes. Using Boolean operations between the geometric solid models of the intact hip joint and the modular stems, the entire hip joint model after THR is constructed (see [15]). During this process, we fabricated solid models of stem head, cup, and liner that are suitable for the modular stems. In particular, we disregarded the fin type thin extrusion of each stem during their solid modeling to reduce the complexity. Also, we prepared not only modular stem models but also the models of the unitary stem with circular or rectangular cross-sections that does not have joints and separable parts. The unitary stem models had the same sizes as the modular stems and were used for comparing the computational results.

2.5. Finite element modeling

Compatible 3D finite element meshes were generated directly in the complete solid model after iterative calculations using commercial software, Patran version 2005 (M.Sc. software, Santa Ana, CA., USA) (see Fig. 3(a)). For lowering the complexity of modeling, the muscle sets around the hip joint were simplified greatly based on the muscle paths [16,17]. Only four muscle paths of gluteii and adductor muscles were modeled for preventing implausible deformations of the hip joint and attached directly to the corresponding nodes on the coxal bone and cortical bone. Linear spring elements with two nodes were used for the muscle paths and quadratic tetrahedral elements with 10 nodes were used for the models of the whole bone and the prosthesis. (Average element and node numbers that were used for all models were 113, 002 and 169, 850, respectively.)

2.6. Material properties and boundary conditions

The relevant materials, such as the cortical and cancellous bones of the bony structures, the articular cartilages, and the liner and the head of the prosthesis were assumed to be isotropic and linear-elastic [18–20]. The gluteii and adductor muscles were considered as linear spring [21]. The materials for the cup and the stem were assumed to be isotropic and elastic-plastic with a power-law hardening exponent of three [15,22]. A biocompatible material, Ti alloy (Ti-6Al-4V), was selected for the cup and the stem (see Table 1).

In terms of boundary conditions for the computations, the degrees of freedom in the x , y , and z -directions were constrained at the nodes on the distal end of the femur. At the nodes on the symmetric surfaces of the sacrum and coxal bones, a constraint

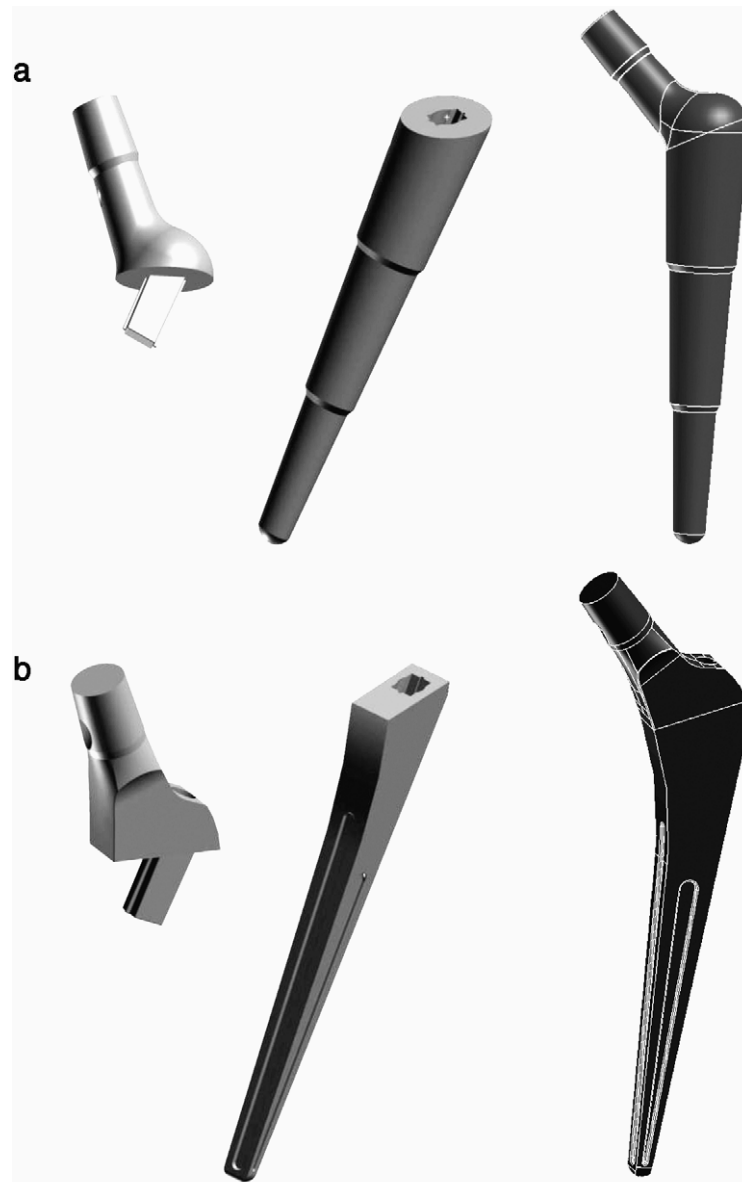


Fig. 1. Solid models of the hip prosthesis with a modular stem: (a) stem with a circular cross-section and (b) stem with a rectangular cross-section.

was applied in the x -direction. On the base of sacrum and the facet of a sacral horn, a load for a single leg stance condition that was three times a woman's weight, viz., 1764 N, was applied; this load was transmitted through the L5 lumbar vertebrae and disc to the sacrum (see Fig. 3(b)). The cup was assumed to be fixed perfectly on the coxal bone. Further, the contact surfaces between the cup and the liner and between the head and the stem were tied perfectly with each other. The frictionless-contact condition was applied between the liner and the stem head. To model a cementless femoral stem, a frictional-contact condition with a frictional coefficient of 0.4 [23] was assumed for the contact surfaces between the stem and the cancellous bone. This frictional coefficient brings about the shear stress on the contact surfaces, which can be a resistant force to the improper subsidence of the stem during numerical calculation. Also, to model the interference fit of the upper and lower part of the modular stem, the contact condition without relative slips between the outer surfaces of the protrusion and the inner surfaces of the cavity was applied because relative micromotions between the two parts must be prevented in real modular stems. However, the frictionless contact condition

was assumed for the contact surface between the upper and the lower part.

3. Results

A commercial software package, ABAQUS version 6.6 (Dassault systems, SIMULIA, RI, USA), was used for the computations. First, mesh convergence tests were carried out using two different FE models with 80% and 120% mesh densities of the present model. The test results show that there are no differences in von Mises stress distributions in each stem and less than 2% difference in its maximum values. Through these tests, the suitability of mesh density of the present model was confirmed.

The obtained von Mises stress distribution of the replaced hip joint using the modular stem with a circular cross-section is shown in Fig. 4(a). The stress values above 10 MPa are seen in the medial and distal regions of the cortical bone of the femur and the maximum value of the stress in the entire model is 571.8 MPa in the cortical bone. The stress distributions for

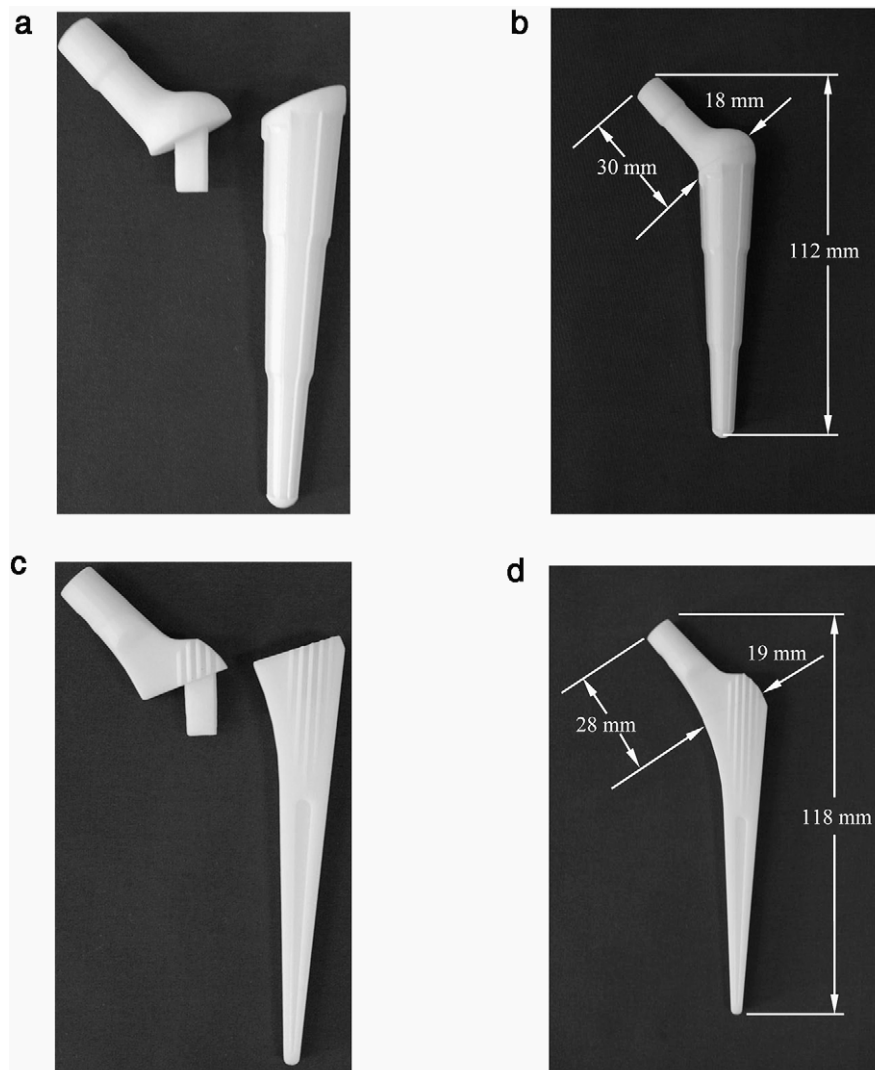


Fig. 2. The modular stem models fabricated using the rapid prototyping machine: (a) and (b) stems with circular cross-sections; (c) and (d) stems with rectangular cross-sections.

the upper and lower parts of the modular stem are shown in Fig. 4(b). We can see that the region just above the shoulder in the upper part and the medial region below the shoulder in the lower part experience high levels of stress (greater than 100 MPa). Interestingly, the stress levels in the protrusion and in the cavity of each part are very low even though those components help to integrate both parts. Because the interference fit between the protrusion and in the cavity was modeled as the contact condition without relative slips, the condition gives both parts continuous displacements. Therefore, this is the reason for the low stress levels in the protrusion and cavity. These low stress levels will be an advantage of the modular stem that is devised in this research. The maximum value of the stress is 185.6 MPa in the upper part and 111.0 MPa in the lower part. Fig. 4(c) shows the stress field in the cancellous bone. The stress values that are higher than 1.0 MPa are found around the resected region of the cancellous bone and the maximum stress value in the cancellous bone is 48.84 MPa.

Fig. 5(a) shows the stress distribution of the replaced hip joint using the modular stem with a rectangular cross-section. The maximum value of the stress over the entire model is 505.2 MPa in the cortical bone. The stress distributions for the upper and lower parts of the modular stem are shown in Fig. 5(b). The region

just above the shoulder in the upper part and the region below the shoulder in the lower part experience high levels of stress. The maximum value of the stress is 156.7 MPa in the upper part and 143.1 MPa in the lower part. Similar to the previous case, the stress levels in the protrusion and the cavity of each part are very low. Fig. 5(c) shows the stress distribution in the cancellous bone. The maximum stress value in the cancellous bone is 43.5 MPa.

To compare the effects of modular stems with those of unitary stems, the stress distributions of the replaced hip joint using the unitary stems are presented in Figs. 6 and 7. The material properties used, the applied load, and the boundary conditions for the computations were the same as those of the cases of modular stems. As shown in Fig. 6(a), the maximum value of the stress around the replaced hip joint using the unitary stem with a circular cross-section is 574.4 MPa in the cortical bone. The stress distribution in the unitary stem with a circular cross-section is shown in Fig. 6(b). A high level of stress is found in the region around the stem neck, which is similar to the case of the modular stem with a circular cross-section. The maximum stress in the stem is 185.7 MPa. Fig. 6(c) shows the stress distributions in the cancellous bone. The maximum stress value in the cancellous bone is 23.8 MPa.

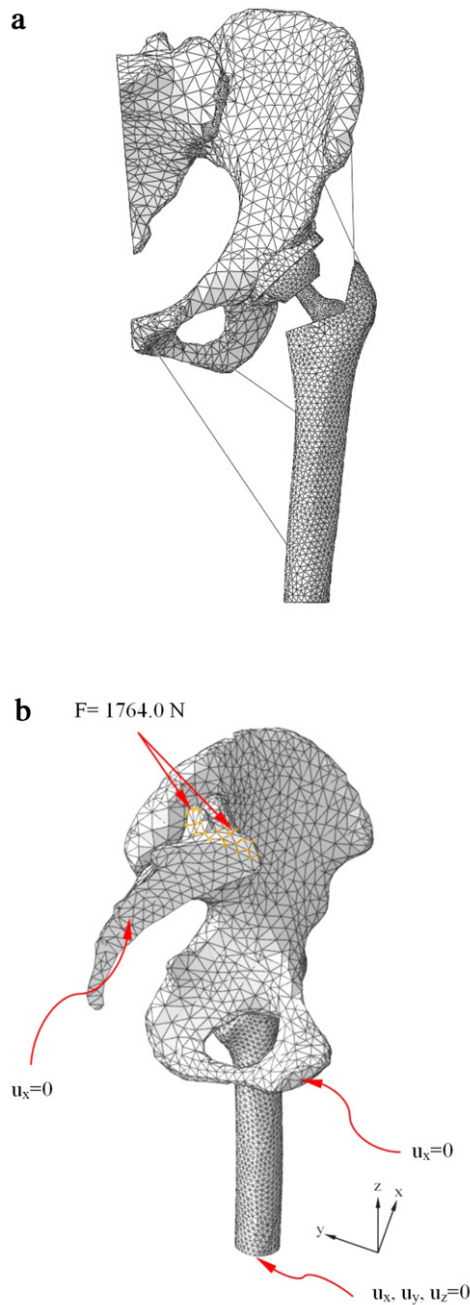


Fig. 3. (a) Finite element model of the hip joint after THR and (b) applied boundary condition.

The stress distribution of the replaced hip joint using the unitary stem with a rectangular cross-section is shown in Fig. 7(a). The maximum value of the stress around the hip joint is 418.3 MPa in the cortical bone. The stress distribution in the unitary stem with a rectangular cross-section is shown in Fig. 7(b). The stress level and the stress distribution are almost similar to those of the case of the modular stem with a rectangular cross-section. The maximum stress in the stem is 155.2 MPa. The maximum stress value in the cancellous bone is 41.82 MPa as shown in Fig. 7(c).

4. Discussion

For all the four cases, the maximum stress value in each part is tabulated in Table 2, with the following terminology: MSS (Maximum von Mises stress in the stem); MSCA (Maximum

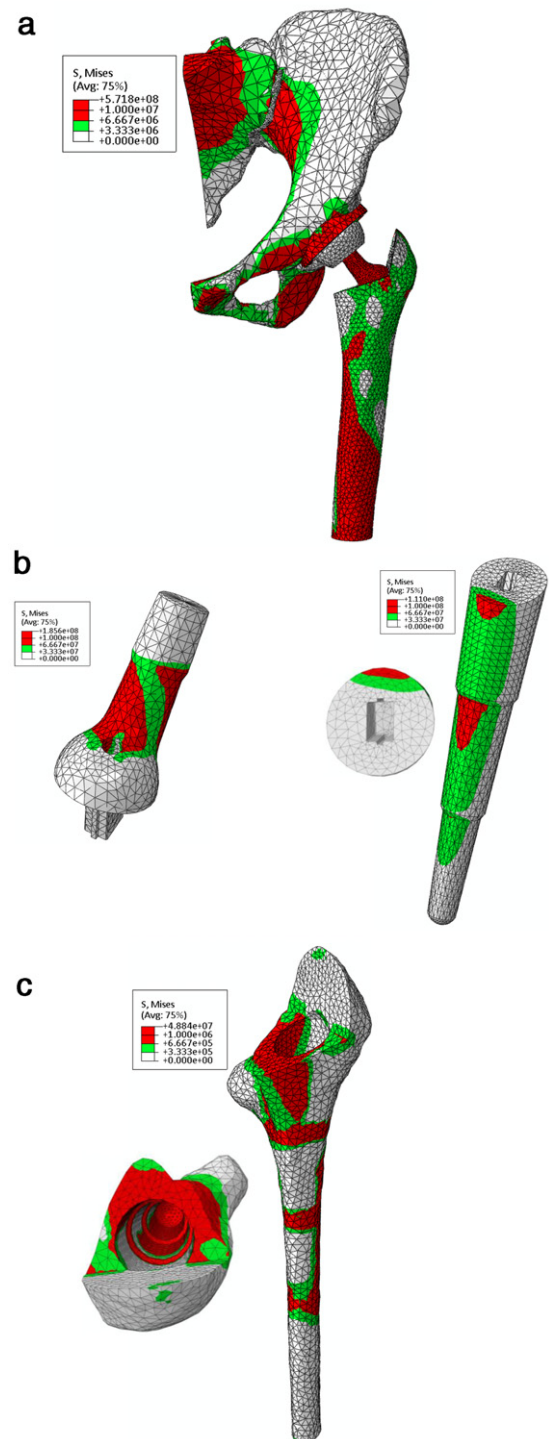


Fig. 4. Von Mises stress distribution in: (a) the replaced hip joint using the modular stem with a circular cross-section, (b) the upper part and the lower part of the modular stem, and (c) the cancellous bone.

von Mises stress in the cancellous bone); MSCO (Maximum von Mises stress in the cortical bone). From Table 2, it is found that the maximum stresses in modular and unitary stems with the same cross-sectional geometry are almost similar. Moreover, the maximum stress is slightly greater in stems with rectangular cross-sections than in stems with circular cross-sections but these values are still much lower than the yield strength of the Ti alloy, viz., 970 MPa. However, the effects of the modular and unitary stems on the stress levels of the cancellous and cortical

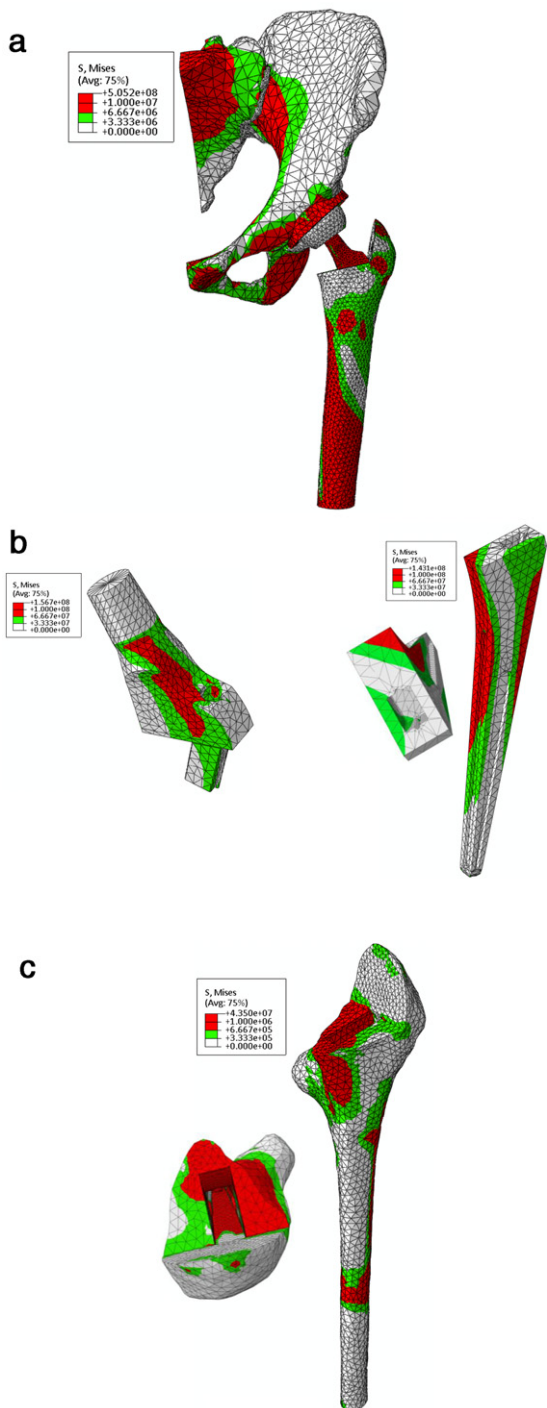


Fig. 5. Von Mises stress distribution in: (a) the replaced hip joint using the modular stem with a rectangular cross-section, (b) the upper part and the lower part of the modular stem, and (c) the cancellous bone.

bones are somewhat different. Under the modular stem with a circular cross-section, the maximum stress in the cancellous bone is about 20 MPa greater than that under the unitary stem with a circular cross-section. Under the modular stem with a rectangular cross-section, the maximum stress in the cortical bone is about 90 MPa greater than that under the unitary stem with a rectangular cross-section. In fact, these differences arise from the geometric differences between the modular and unitary stems. However, these differences are regarded as small differences that easily can be reduced by optimizing the shape of the stem.

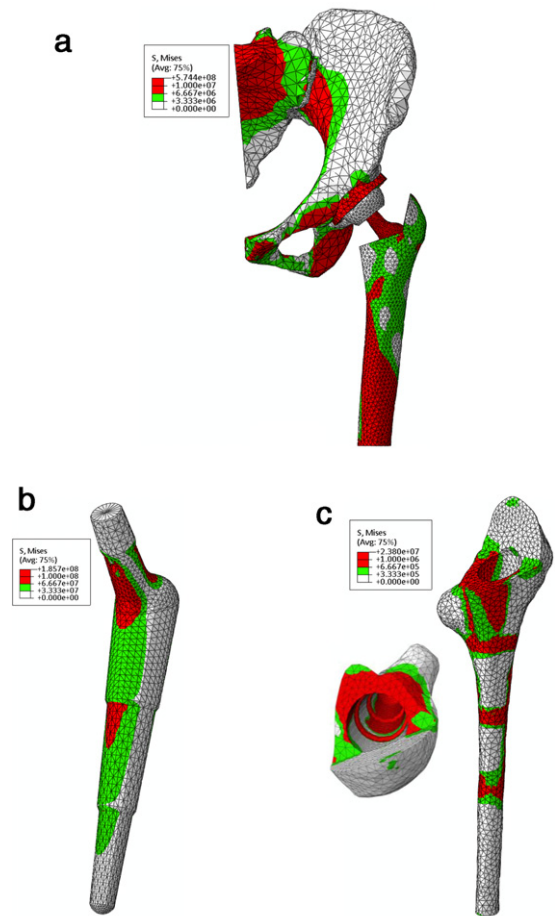


Fig. 6. Von Mises stress distribution in: (a) the replaced hip joint using the unitary stem with a circular cross-section, (b) the unitary stem, and (c) the cancellous bone of the femur.

Table 2

The maximum value of the von Mises stress in different parts of the replaced hip joint under all four geometries of the stem.

Cases	MSS (MPa)	MScA (MPa)	MScO (MPa)
Modular stem with a circular cross-section	185.6 (Upper part) 110.0 (Lower part)	48.84	571.8
Modular stem with a rectangular cross-section	156.7 (Upper part) 143.1 (Lower part)	43.5	505.2
Unified stem with a circular cross-section	185.7	23.8	574.4
Unified stem with a rectangular cross-section	155.2	41.82	418.3

Based on these computational results, we can validate our idea of developing a modular stem for minimally invasive THR and fabricate various sizes of actual modular stems with circular or rectangular cross-sections using the biocompatible Ti alloy (Ti-6Al-4V) and a machining center, M2 3AX/5AX of WHACHEON, Co. Ltd (see Fig. 8). These fabricated specimens actually will be used in the near future by orthopedic surgeons.

5. Conclusions

Cementless modular stems with circular or rectangular cross-sections for minimally invasive THR are suggested and validated based on Bio-CAD modeling technique and finite element analysis. In particular, two unitary stems with circular or rectangular cross-sections also are modeled and used for the computations for the

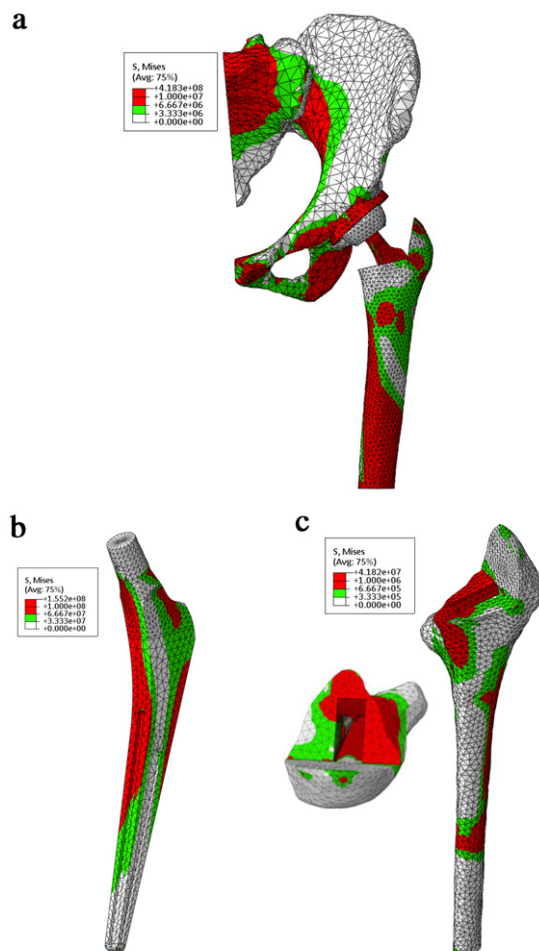


Fig. 7. Von Mises stress distribution in: (a) the replaced hip joint using the unitary stem with a rectangular cross-section, (b) the unitary stem, and (c) the cancellous bone of the femur.

sake of comparison. From the results, it is found that the von Mises stress level and the von Mises stress distributions in modular and unitary stems with the same cross-sectional geometry are almost similar. Moreover, the maximum stress is slightly greater in stems with rectangular cross-sections than in stems with circular cross-sections. However, all the maximum stress values are much smaller than the yield stress (970 MPa) of the material used. This means that we can use the modular stem for THR within the safe limit before yielding occurs. Depending on the cross-sectional geometry of the stems, the maximum stress values in the cancellous and/or cortical bones under the modular stems are greater than those under the unitary stems. The maximum differences are about 20 MPa for the cancellous bone and 90 MPa for the cortical bone, respectively. However, it is thought that these differences can easily be reduced by the optimal design of the shape of the modular stem.

Based on the computational results, various sizes of actual modular stems with circular or rectangular cross-sections are fabricated using a biocompatible Ti alloy (Ti-6Al-4V). These stems facilitate minimally invasive THR for the concerned operating surgeons. Therefore, they will be used in the near future.

Acknowledgments

I. Jeon thanks Mr. Jinhong Park, Sangjin Song and Sintae Kang of Chonnam National University for their work on the geometric modeling of a hip joint. This work is supported by the Nuclear

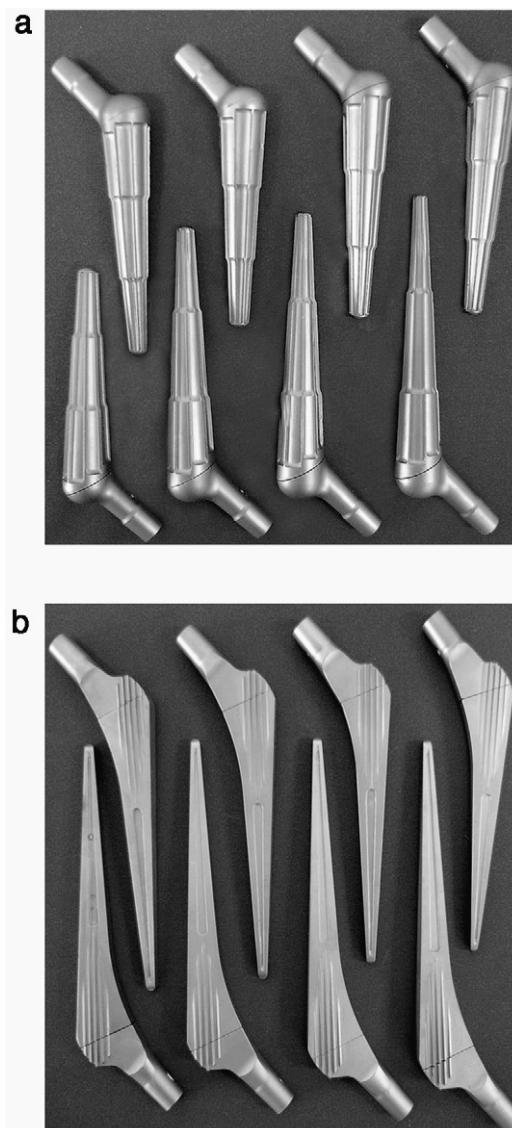


Fig. 8. Fabricated actual modular stems of Ti alloy (Ti-6Al-4V) with various sizes of (a) circular and (b) rectangular cross-sectioned stems.

R&D Program through the National Research Foundation of Korea funded by the Ministry of Education, Science and Technology (Grant No. 2008-2006034).

References

- [1] Bal BS, Haltom D, Aleto T, Barrett M. Early complications of primary total hip replacement performed with a two-incision minimally invasive technique. *J Bone Joint Surg Am* 2005;87:2432–8.
- [2] Glaser D, Dennis DA, Komistek RD, Miner TM. In vivo comparison of hip mechanics for minimally invasive versus traditional total hip arthroplasty. *Clin Biomech (Bristol, Avon)* 2008;23:127–34.
- [3] Howell JR, Masri BA, Duncan CP. Minimally invasive versus standard incision anterolateral hip replacement: a comparative study. *Orthop Clin N Am* 2004;35:153–62.
- [4] Ong KL, Kurtz SM, Manley MT, Rushton N, Mohammed NA, Field RE. Biomechanics of the Birmingham hip resurfacing arthroplasty. *J Bone Joint Surg Br* 2006;88:1110–5.
- [5] Stolk J, Verdonchot N, Cristofolini L, Toni A, Huiskes R. Finite element and experimental models of cemented hip joint reconstructions can produce similar bone and cement strains in pre-clinical tests. *J Biomech* 2002;35:499–510.
- [6] Mathias KJ, Leahy JC, Heaton A, Deans WF, Hukins DW. Hip joint prosthesis design: effect of stem introducers. *Med Eng Phys* 1998;20:620–4.
- [7] Goetzen N, Lampe F, Nassut R, Morlock MM. Load-shift-numerical evaluation of a new design philosophy for uncemented hip prostheses. *J Biomech* 2005;38:595–604.

- [8] Namba RS, Keyak JH, Kim AS, Vu LP, Skinner HB. Cementless implant composition and femoral stress. A finite element analysis. *Clin Orthop Relat Res* 1998;347:261–7.
- [9] Barrack RL. Modularity of prosthetic implants. *J Am Acad Orthop Surg* 1994;2: 16–25.
- [10] Bono JV. S-ROM modular total hip replacement. *Oper Tech Orthop* 2001;11: 279–87.
- [11] Helm CS, Greenwald AS. The rationale and performance of modularity in total hip arthroplasty. *Orthopaedics* 2005;28:s1113–5.
- [12] Sun W, Starly B, Nam J, Darling A. Bio-CAD modeling and its applications in computer-aided tissue engineering. *Comput Aided Des* 2005;37: 1097–1114.
- [13] Tuan HS, Huttmacher DW. Application of micro CT and computation modeling in bone tissue engineering. *Comput Aided Des* 2005;37:1151–61.
- [14] Weeden BA, Sanders AP, LaSalle DL, Trottier GP. Alternative methods for custom implant production utilizing a combination of rapid prototyping technology and conventional investment casting. In: *Biomedical engineering conference. Proceedings of the 1996 fifteenth southern*. 1996. p. 555–7.
- [15] Jeon I, Bae JY, Park JH, Yoon TR, Todo M, Mawatari M, et al. Biomechanical effect of the collar of femoral stem on total hip arthroplasty. *Comput Methods Biomech Biomed Eng* 2011;14:103–12.
- [16] Bitsakos C, Kerner J, Fisher I, Amis AA. The effect of muscle loading on the simulation of bone remodelling in the proximal femur. *J Biomech* 2005;38: 133–9.
- [17] Speirs AD, Heller MO, Duda GN, Taylor WR. Physiologically based boundary conditions in finite element modelling. *J Biomech* 2007;40:2318–23.
- [18] Kempson GE. The mechanical properties of articular cartilage. Sokoloff L, editor. *The joints and synovial fluid*, vol. 2. New York: Academic Press; 1980. p. 177–238.
- [19] Kopparti PSarathi, Lewis G. Influence of three variables on the stresses in a three-dimensional model of a proximal tibia-total knee implant construct. *Biomed Mater Eng* 2007;17:19–28.
- [20] Mak M, Besong A, Jin Z, Fisher J. Effect of microseparation on contact mechanics in ceramic-on-ceramic hip joint replacements. *Proc Inst Mech Eng, Part H: J Eng Med* 2002;216:403–8.
- [21] Phillips AT, Pankaj P, Howie CR, Usmani AS, Simpson AH. Finite element modelling of the pelvis: inclusion of muscular and ligamentous boundary conditions. *Med Eng Phys* 2007;29:739–48.
- [22] Jeon I, Katou K, Sonoda T, Asahina T, Kang K-J. Cell wall mechanical properties of closed-cell Al foam. *Mech Mater* 2009;41:60–73.
- [23] Rancourt D, Shirazi-Adl A, Drouin G, Paiement G. Friction properties of the interface between porous-surfaced metals and tibial cancellous bone. *J Biomed Mater Res* 1990;24:1503–19.